Effects of Working Fluid Filling Ratio and Heat Flux on Correlations of Heat Transfer Coefficient in Loop Thermosyphon

Ki-Chang Chang* and Young-Soo Lee*

Key words: Loop thermosyphon, Working fluid filling ratio, Distilled water, Carbon-steel, Heat transfer coefficient

Abstract

Due to the coupling between momentum and energy transport theoretical analysis of the loop performance is very complicate, therefore it is necessary that these problems be solved by experimental investigation before applying the loop thermosyphon to heat exchanger design. The evaporator and condenser of the loop thermosyphon were made of carbon-steel, and distilled water was used as working fluid in the experiments. From the experimental data correlations of heat transfer coefficient for evaporator and condenser sections were obtained. For heat fluxes in the range of 13000~78000 W/m^2, the correlation equations of heat transfer coefficients in evaporator and condenser predict the experimental behavior to within ±5% and ±20% respectively.

Nomenclature

A : area [m^2]
c_p : specific heat [kJ/kg K]
d_i : inner diameter [m]
G : mass flow rate [kg/s]
Gr : Grashof number, $\frac{\beta g \Delta T d_i^3 \rho_r^2}{\mu^2}$
h : heat transfer coefficient [W/ m^{2}K]
H : height [m]
f : friction factor
L : length of loop [m]
L_{ec} : effective length [m]
Nu : Nusselt number, $\frac{hd_i}{k}$
P_{sat} : saturation vapor pressure [Pa]
Pr : Prandtl number, $\frac{\mu c_p}{k}$
q : heat flux [W/m^2]
R : working fluid filling ratio, H_l/H_0
t : time [s]
T : temperature [℃]
T_w : wall temperature [℃]
V : velocity [m/s]

* Unutilized Energy Research Team, Korea Institute of Energy Research, Taejon 305-343, Korea

Greek symbols

β : thermal expansion coefficient [1/℃]
μ : density [kg/m^3]
ρ : absolute viscosity [kg/m s]
σ : surface tension [N/m]
τ_w : shear stress [kg/m^2]

Subscripts

c : condenser
e : evaporator
i : inside
o : outside
v : vapor
l : liquid
ss : steady state

1. Introduction

The loop thermosyphon transports thermal energy from a heat source to a sink by natural convective circulation without any external power supply such as a pump. An evaporator and a condenser are installed separately, but these are connected to each other by circulating tubes. Since the loop thermosyphon has larger critical heat flux than conventional thermosyphon due to the same directions of the flows of vapor and liquid,[1] it is widely used in many applications, such as cooling of power electronic components, heat removal of nuclear power plant, solar heating and cooling system, geothermal power generation, waste heat recovery system and so on.[2]

In the loop thermosyphon, various types of flow instabilities occur depending on the system geometry, the working fluid filling ratios and the operating conditions, and often lead to abnormal behavior such as limit cycle oscillations or premature dry-out. Due to the coupling between momentum and energy transport theoretical analysis of the loop performance is very complicate, therefore it is necessary that these problems be solved by experimental investigation before applying the loop thermosyphon to heat exchanger design.[3,4]

Loop thermosyphon is a heat transfer device of very high thermal conductance in which fluid circulates. The heat transfer is considered to be affected by many factors, such as working fluid, quantity of the working fluid, inside pipe diameter, pipe length, ratio of cooled surface to heated surface, adiabatic length between heated and cooled sections, heat flux and operating temperature.

There are some papers related flow instability and heat transfer characteristics according to working fluids, but it has not studied dimensionless heat transfer coefficients depending on the variation of working fluids, filling ratios and heat flux. In the present study, the evaporator and condenser of the loop thermosyphon were made of carbon-steel. Water was used as working fluid in the experiments. From the experimental data a reasonable filling ratio of working fluid and heat transfer coefficients for evaporator and condenser sections were obtained. In order to establish heat transfer correlations for the application in the design program for the loop thermosyphon heat exchanger, regression analysis was applied to experimental data for heat transfer coefficients in evaporator and condenser.

2. Analysis of heat transfer

As shown in Fig. 1, it is assumed that a constant and uniform heat flux q_e is supplied in the evaporator section, while heat is removed from the loop in the condenser section. The loop is divided into six sections, such as adiabatic liquid phase (①~②), heating liquid phase (②~③), heating two-phase (③~④), adiabatic two-phase (④~⑤), cooling two-phase (⑤~⑥) and cooling liquid phase (⑥~①). Where,

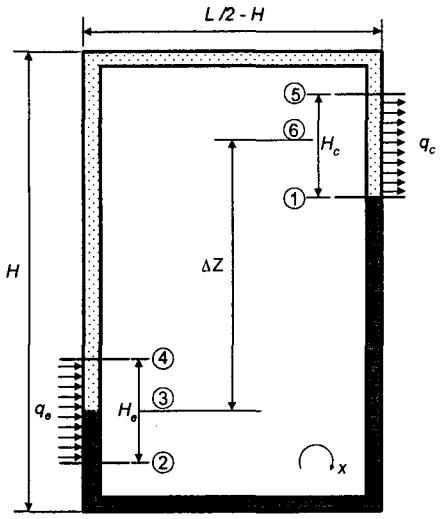

Fig. 1 Configuration and coordinate system of loop thermosyphon.

the position ③ is the boundary of liquid and vapor in evaporator, and the position ⑥ is the boundary of liquid and vapor in condenser when loop thermosyphon is operated in steady state. The axial conduction heat transfer along the pipe wall and in the working fluid was negligible in comparison with convection, and heat loss from the loop to the ambient was neglected.[5]

Application of the conservation of mass, momentum and energy for one-dimension buoyancy-driven flow about the loop gives governing differential equations, and it is noted that the shear force relation $\tau_w = f\rho_r V^2/2$. Therefore the non-dimensional differential equations are obtained following set, using non-dimensional temperature $\theta = (T - T_r)/(q/h)$, non-dimensional velocity $V^* = V/V_r$, non-dimensional time $\tau = V_r t/L$, and non-dimensional length $S = x/L$.[6]

$$V^* = V^*(\tau) \tag{1}$$

$$\frac{\partial V^*}{\partial \tau} + 2f\left(\frac{L_{ec}}{d_i}\right)V^{*2} = \mathrm{St}\int_0^1 \theta dS\, \dot{e}_z \cdot \dot{e}_x \tag{2}$$

$$\frac{\partial \theta}{\partial \tau} + V^*\frac{\partial \theta}{\partial S} = \frac{4\mathrm{St}}{(d_i/L)}, \quad 0 \le S \le \frac{H_e}{L} \tag{3}$$

$$\frac{\partial \theta}{\partial \tau} + V^*\frac{\partial \theta}{\partial S} = -\frac{4\mathrm{St}}{(d_i/L)}, \quad \frac{1}{2} \le S \le \frac{1}{2} + \frac{H_c}{L} \tag{4}$$

$$\frac{\partial \theta}{\partial \tau} + V^*\frac{\partial \theta}{\partial S} = 0 \tag{5}$$

Where, St is the Stanton number defined as

$$\mathrm{St} = \frac{h}{\rho_r c_p V_r} = \frac{h^3}{qLg\beta(\rho_r c_p)^2} \tag{6}$$

V_r is a reference velocity defined as

$$V_r = \frac{qLg\beta\rho_r c_p}{h^2} \tag{7}$$

By solving equation (3) with vanishing time derivative terms, a steady-state linear temperature solution is obtained in the evaporator section.

$$\theta_{ss} = \theta_{2ss} + \frac{4\mathrm{St}}{V_{ss}^*(d_i/L)}S, \quad 0 \le S \le \frac{H_e}{L} \tag{8}$$

Similarly, solution of equation (4) yields distribution in the condenser section.

$$\theta_{ss} = \theta_{5ss} - \frac{4\mathrm{St}}{V_{ss}^*(d_i/L)}\left(S - \frac{1}{2}\right), \quad 0 \le S \le \frac{H_c}{L} \tag{9}$$

Equation (5) gives a uniform temperature solution for the insulated parts of the loop, i.e., $\theta_{1ss} = \theta_{2ss}$ and $\theta_{4ss} = \theta_{5ss}$. Here, a characteristic temperature difference of the loop can be defined and determined from equations (8) and (9).

$$\theta_{4ss} - \theta_{2ss} = \frac{4\mathrm{St}(H_e/L)}{V^{*ss}(d_i/L)} \tag{10}$$

$$\theta_{1ss} - \theta_{5ss} = -\frac{4\mathrm{St}(H_c/L)}{V^{*ss}(d_i/L)} \tag{11}$$

The temperature distributions solved previously can then be substituted into the integral term of the momentum equation (2), to yield following set.

Solving the above algebraic equations, the circulating velocity of the loop thermosyphon at steady-state can be obtained.

$$V_{ss}^{*3} = \frac{\mathrm{St}^2(H_e/L)}{f(L_{ec}/L)} \tag{12}$$

Here, a conventional correlation for friction factor at steady state is used, which is in the form $f = n/\mathrm{Re}_{ss}^{m}$, where Re_{ss} is the Reynolds number defined at steady state, i.e., $\mathrm{Re}_{ss} = \rho_r d_i V_{ss}^{*}/\mu$, and n and m are equal to 16 and 1, respectively, for laminar flow, and 0.079 and 0.25, respectively, for turbulent flow. Substituting this into equation (12), it can be shown that in the following relations, the characteristic parameter WY is obtained.

$$\mathrm{Re}_{ss} = \left(\frac{WY}{16}\right)^{\frac{1}{2}} \quad : \text{laminar flow} \tag{13}$$

$$\mathrm{Re}_{ss} = \left(\frac{WY}{0.079}\right)^{\frac{1}{7}} \quad : \text{turbulent flow} \tag{14}$$

Where W is a non-dimensional parameter related to the heat flux q, which is defined as

$$W \equiv \frac{\rho_r^2 g\beta d_i^4 q}{\mu^3 c_p} \tag{15}$$

Y is geometric non-dimensional parameter defined as

$$Y \equiv \frac{(H_e/L)}{(d_i/L)(L_{ec}/L)} \tag{16}$$

It is worthwhile noting that the parameter W defined in equation (15) can be written in terms of the Nusselt number of the heater and Grashof and Prandtl numbers (Gr and Pr)

$$W = \mathrm{NuGr/Pr} \tag{17}$$

In this case, equation (13) and (14) can be treated as a theoretical convective heat transfer correlation for the loop thermosyphon and can be converted into the form

$$\begin{aligned} &(\mathrm{NuGr/Pr})Y = 16\mathrm{Re}_{ss}^{2} \quad \text{for laminar flow} \\ &(\mathrm{NuGr/Pr})Y = 0.079\mathrm{Re}_{ss}^{\frac{1}{7}} \quad \text{for turbulent flow} \end{aligned} \tag{18}$$

Therefore the correlation $\mathrm{Nu} = f(\mathrm{Re}_{ss})$ can be used. If it is defined as $X = WY$, dimensionless heat transfer coefficient is as follows.

$$\begin{aligned} \mathrm{Nu} &= f(\mathrm{Re}_{ss}) \\ &= f(WY) = f(X) \\ &= aX^{b} \ (a \text{ and } b \text{ are constants}) \end{aligned} \tag{19}$$

3. Experimental apparatus and procedure

In the present study, an experimental apparatus was constructed and measurements were made to study the steady and transient natural circulation phenomena and determine the heat transfer coefficients evaporator and condenser section that is to be used in dimensionless analysis.

Shown schematically in Fig. 2 is the loop thermosyphon used in the experiments. The evaporator and condenser of loop thermosyphon were composed of tubing of 20.3 mm inner diameter with 300 mm length, made of carbon-steel, respectively. The loop was made of stainless steel in a rectangular shape with a 7.75 mm inner diameter, a height 1.7 m and a width 1.0 m. The relative height between the evaporator and condenser measured from their cen-

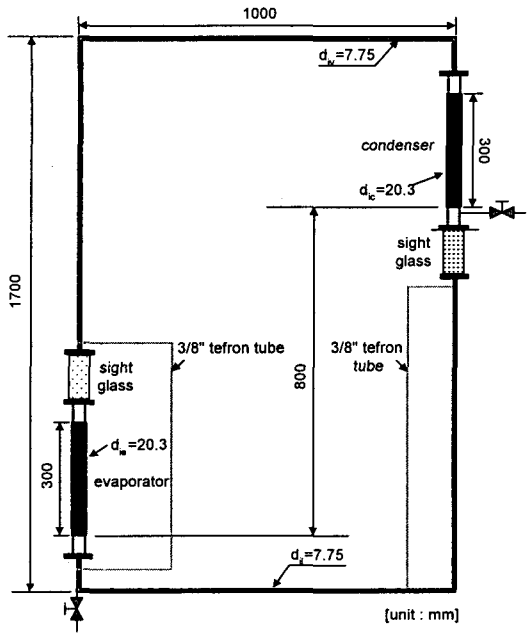

Fig. 2 Schematic of loop thermosyphon.

ters is 0.8 m.

The evaporator of the loop was provided directly by a constant and uniform heat flux by an evenly wound shielded electrical heating wire attached tightly on the evaporator surface. The condenser of the loop was provided by the cooling jacket using water as the coolant to remove heat from the loop. The vertical cooler of the loop was designed as a double-pipe heat exchanger consisting an annular jacket connected to a constant temperature bath with coolant flowing in the upward direction, as schematically shown in Fig. 3.

Distilled water was the working fluid. The electrical heat was supplied to the evaporator through a variable transformer (range 0~3000 W) and was measured with watt transducer. To reduce the heat loss to the ambient, the heater was insulated by 50 mm-thick ceramic fiber (k=0.090636 W/mK). To prevent heat loss in condenser and line, 25 mm-thick ceramic fiber insulation was installed over the outside surface of the cooler and the connecting pipes. The total heat loss was found to be approximately 5% of the total heat input, which was determined by measuring the heat input power in the evaporator and the cooling rate in the condenser.

In order to investigate the flow of working fluid the sight glasses were installed upper evaporator and below condenser, respectively, and in order to measure filling ratio of work-

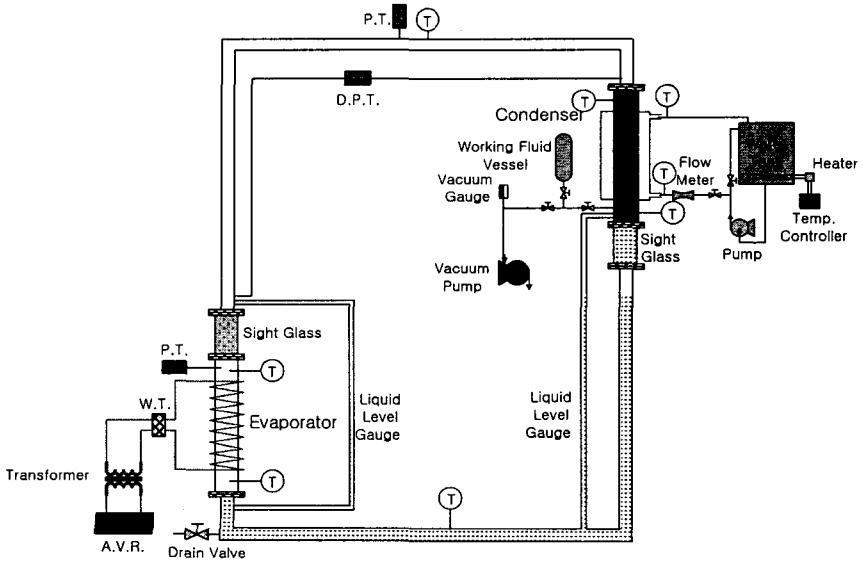

Fig. 3 Schematic of experimental apparatus for loop thermosyphon.

ing fluid the visible tefron tube with 9.53 mm outside diameter was installed on liquid line.

To measure the temperature distribution the loop was installed with a total of 18 K-type thermocouples, 6 thermocouples were inserted inside connecting tube, 7 thermocouples were attached on the surface of evaporator, and 5 thermocouples were attached on the surface of condenser. To measure saturation pressure of working fluid and pressure drop in vapor line, pressure transducer (range 0~202 kPa) and differential pressure transducer (range 0~20 kPa) were installed respectively. The measuring data were recorded by Data Acquisition System.

The experimental procedure was as follows. The filling ratios of working fluid were 30, 40, 50, 70, 90, 110% of evaporator volume, and the heat transfer rates of evaporator were 250, 500, 750, 1000, 1250, 1500 W, respectively. The coolant flow rate was constantly 500 L/h, but when the saturation vapor temperature was 60, 70, 80℃, the coolant temperature and flow rate were varied.

The heat transfer coefficients of evaporator and condenser are calculated by the experimental value, the procedure is as follows.[7]

$$\overline{T_{wo}} = \frac{1}{A_o}\int T_{wo}\,dA \tag{20}$$

$$T_{wi} = \overline{T_{wo}} - \frac{Q\ln(r_o/r_i)}{2\pi kL} \tag{21}$$

$$\mathrm{Nu} = \frac{q}{|(T_w - T_{sat})|}\frac{d_i}{k} \tag{22}$$

4. Results and discussion

4.1 Correlation of heat transfer coefficient in evaporator

The steady-state performance was measured using the experimental loop, and the heat transfer coefficient in evaporator was obtained. The parameter W appearing in equation (15) can be experimentally determined by measuring the heat flux q in the evaporator, the parameter Y appearing in equation (16) can be determined by geometric lengths.[8] The heat transfer coefficient in evaporator is defined by the function of X using W and Y, it is shown

$$\mathrm{Nu}_e = aX_e^b \tag{23}$$

Figure 4 shows that the measured heat transfer coefficient is the largest value in filling ratio 50%, when it was operated in varying heat flux with constant saturation pressure 4800 Pa. It is shown that the heat transfer coefficient in evaporator decrease with increasing filling ratio. Therefore the heat transfer coefficient also depends on filling ratios, the equation (23) is modified as

$$\mathrm{Nu}_e = aX_e^{b_1}R^{b_2} \tag{24}$$

It is noted the relation of heat transfer coefficient and saturation pressure in Fig. 5. If the heat transfer coefficient increase with increasing X_e, varying saturation pressure in

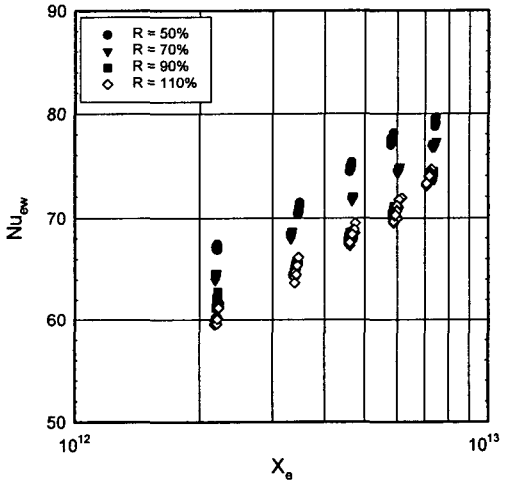

Fig. 4 Dependence of Nu_e in evaporator on dimensionless X_e for various filling ratios (P_{sat}=4800 Pa).

loop nearly has an effect on that. Because the parameter W relating to heat flux includes saturation properties of working fluid, the parameter W varies with varying saturation pressure. Therefore the X_e depends on W, the saturation pressure does not affect the heat transfer coefficient directly. The correlation of heat transfer coefficient represents by both X_e and R.

Figure 6 illustrates the power-law relationship between the dimensionless X_e and Nusselt number, Nu_e based on the heat transfer coefficient in evaporator. The correlation curve was obtained from a least-square regression of

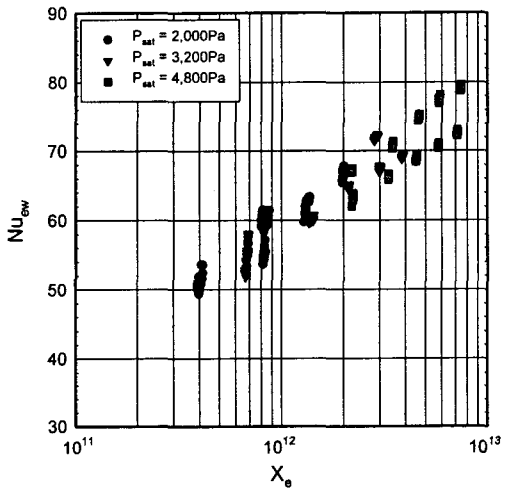

Fig. 5 Dependence of Nu_e in evaporator on dimensionless X_e for various saturation pressures (R=50%).

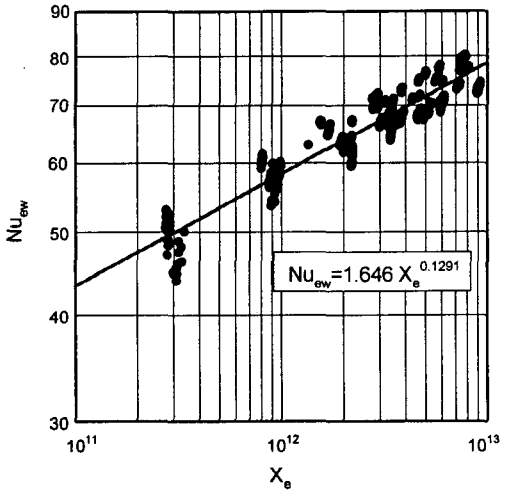

Fig. 6 Correlation of Nu_e as a function of dimensionless X_e in evaporator.

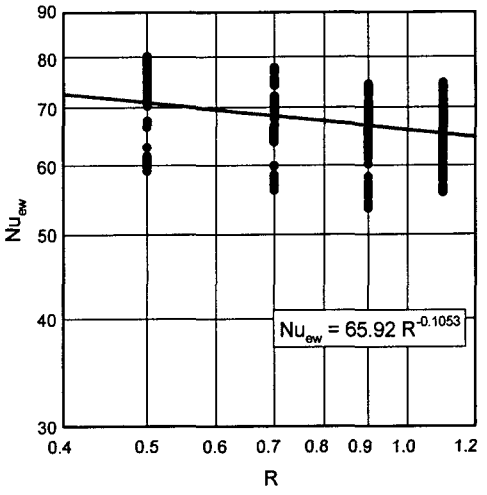

Fig. 7 Correlation of Nu_e as a function of filling ratio R in evaporator.

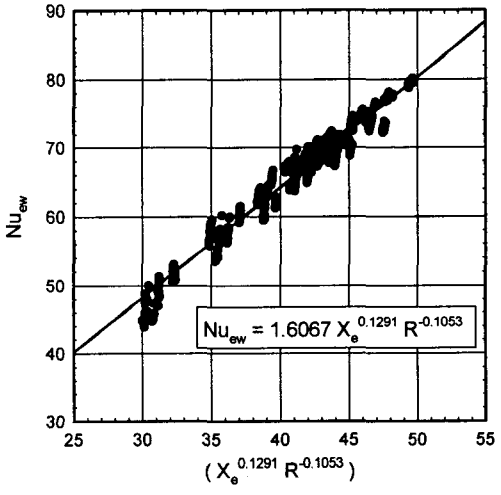

Fig. 8 Correlation of Nu_e in evaporator with eqn. (25).

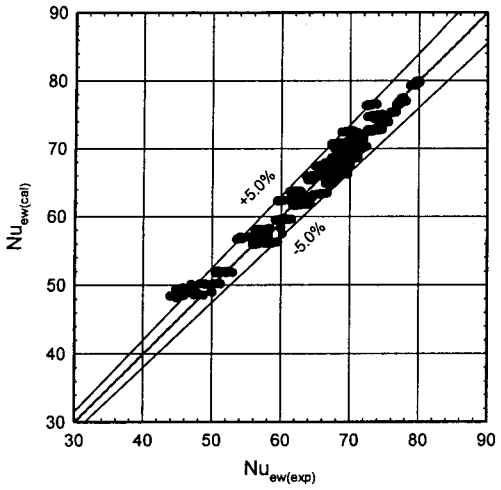

Fig. 9 Comparison of predicted and experimental value in evaporator.

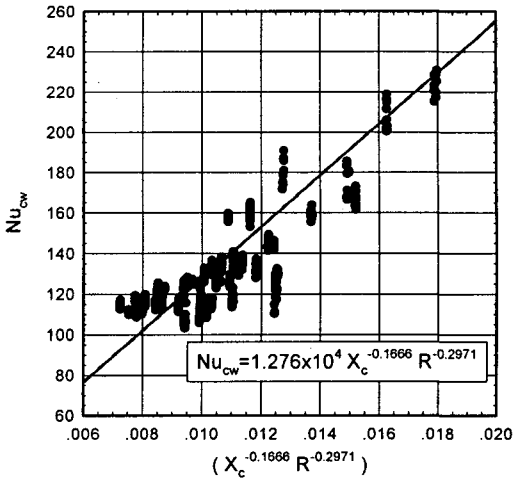

Fig. 10 Correlation of Nu_c in condenser with eqn. (26).

the experimental data, the exponential value was 0.1291. And Fig. 7 illustrates the power-law relationship between the filling ratio R and Nusselt number, the filling ratio R based on the range of heat flux 13000~78000 W/m^2. The heat transfer coefficient decrease with increasing filling ratio, the exponential value resulted in -0.1053.

Figure 8 shows that the relationship between the dimensionless ($X_e^{0.1291}R^{-0.1053}$) and Nu_e are linear, the correlation of heat transfer coefficient was obtained from a least-square regression of the experimental data, which is of the form

$$Nu_{ew} = 1.6067 X_e^{0.1291} R^{-0.1053} \quad (25)$$

Fig. 9 illustrates the comparison of predicted and measured values, the correlation equation of heat transfer coefficient in evaporator predicts the experimental behavior to within 5.0 percents.

4.2 Correlation of heat transfer coefficient in condenser

The heat transfer coefficient in condenser was obtained by the same procedure used in evaporator. According to the power-law relationship between the dimensionless X_c and Nusselt number, Nu_c based on the heat transfer coefficient in condenser. The correlation curve was obtained from a least-square regression of the experimental data, the exponential value was -0.1666. In filling ratio the exponential value resulted in -0.2971. The heat transfer coefficient in condenser decrease with increasing X_c and R.

Figure 10 shows that the relationship between the dimensionless ($X_c^{-0.1666}R^{-0.2971}$) and Nu_c are linear, the correlation of heat transfer coefficient was obtained from a least-square regression of the experimental data, which is of the form

$$Nu_{cw} = 1.276 \times 10^4 X_c^{-0.1666} R^{-0.2971} \quad (26)$$

Figure 11 illustrates the comparison of predicted and measured values, the correlation equation of heat transfer coefficient in condenser predicts the experimental behavior to within 20.0 percents. In addition the correlation included saturation pressure predicts the ex-

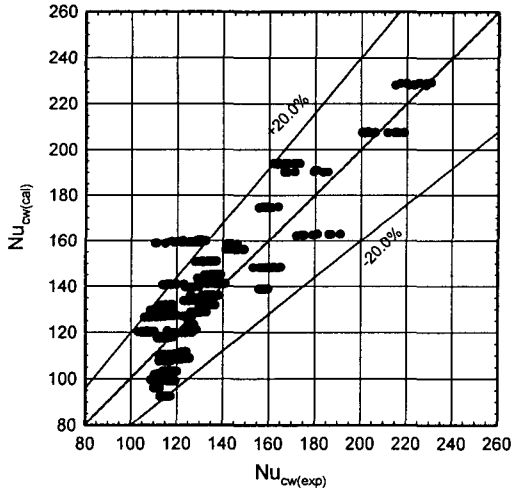

Fig. 11 Comparison of predicted and experimental value in condenser.

perimental behavior to within 30.0 percents, the error of correlation without saturation pressure reduced about 10 percents than that of correlation with saturation pressure.[9] Finally the correlation of heat transfer coefficient in the loop thermosyphon is denoted by complex of dimensionless X and filling ratio R.

5. Conclusions

The results of a combined study of experiment and correlation for steady state heat transfer behavior of the loop thermosyphon have been presented. For the range of heat flux, 13000~78000 W/m^2 the reasonable filling ratio of working fluid is about 50% of the evaporator volume, and the correlation equations for boiling and condensation heat transfer coefficients predict the experimental behavior to within ±5% and ±20% respectively.

The correlations of heat transfer coefficient in evaporator and condenser are respectively as follows;

$$Nu_{ew} = 1.6067 X_e^{0.1291} R^{-0.1053}$$

$$Nu_{cw} = 1.276 \times 10^4 X_c^{-0.1666} R^{-0.2971}$$

References

1. Japkise, D., 1973, Advance in thermosyphon technology, in J. P. Hartnett, T. F. Irvine (eds.), Advances in Heat Transfer, Vol. 9, Academic Press, New York.
2. Zvirin, Y., 1981, A review of natural circulation loops in pressurized water reactors and other systems, Nucl. Engng Des. 67 pp. 203-225.
3. Mertol, A., Place, W., Webster, T. and Greif, R., 1981, Detailed loop model (DLM) analysis of liquid solar thermosyphons with heat exchangers, Solar Energy 27, pp. 367-386.
4. Parent, M. G., Van Der Meer, Th. H. and Hollands, K. G. T., 1990, Natural convection heat exchangers in solar water heating systems: theory and experiment, Solar Energy 45, pp. 43-52.
5. Karl Stephan and Hein Auracher, 1981, Correlation for nucleate boiling heat transfer in forced convection, Int. J. Heat Mass Transfer 24, pp. 99-107.
6. Huang, B. J. and Zelaya, R., 1988, Heat transfer behavior of a rectangular thermosyphon loop, Journal of Heat Transfer Transactions of the ASME 110, pp. 487-493.
7. Chang, K. C., Lee, K. W. and Yoo, S. Y., 1998, Experimental study on the heat transfer characteristics of separate type thermosyphon, Korean Journal of Air-Conditioning and Refrigeration Engineering 10(1), pp. 22-32.
8. Chang, K. C., Lee, K. W. and Yoo, S. Y., 1998, Effects of working fluid filling ratio and heat flux on heat transfer for separate type thermosyphon, Proceedings of the SAREK'98 Winter Annual Conference, pp. 263-268.
9. Chang, K. C., Lee, K. W., Ra, H. S. and Yoo, S. Y., 1999, Correlations of Heat Transfer Coefficient in Separate Type Thermosyphon, Proceedings of the SAREK'99 Summer Annual Conference, pp. 77-83.